SLAC – PUB – 3962
May 1986
(E)

SEARCHES FOR NEW PARTICLES AT PEP*

MICHAEL J. JONKER

Stanford Linear Accelerator Center
Stanford University, Stanford, California 94305

ABSTRACT

The status of searches for new particles at the PEP storage ring is reviewed. The result of the excited electron search by MARKII is presented and a limit on the coupling strength of the $e^*e\gamma$ vertex is given. The search for single photons in the ASP and MAC detectors is reported and the results are used to set limits on the number of light neutrino species and, in the context of supersymmetry (SUSY) theories, are interpreted as setting simultaneous limits on the masses of the selectron and photino.

* Work supported by the Department of Energy, contract DE – AC03 – 76SF00515.

Contributed to the XXIth Rencontre de Moriond: Perspectives in Electroweak Interactions and Unified Theories, Les Arcs, France, March 9-16, 1986

1. Excited Electron Search

This section discusses the search for excited electrons with the MARKII detector. If the electron is composite, an excited state (e^*) can be observed in e^+e^- annihilations provided the mass of the e^* is low enough. Pair production is allowed for $m_{e^*} < \frac{1}{2}\sqrt{s}$. For $m_{e^*} < \sqrt{s}$ the e^* can be produced singly. In either case a signal would be the decay into an $e\,\gamma$ pair with an invariant mass equal to m_{e^*}. Even for $m_{e^*} > \sqrt{s}$, the e^* could be detected by the effect of additional diagrams with e^* propagators on pure QED processes. In all cases the e^* signal competes with a QED background.

This analysis sets a limit on single e^* production by searching for a peak in the invariant mass distribution of $e\gamma$ events. Only the virtual Compton process is studied, i.e. the channel near the pole, $t \to 0$.

QED and e^* Production

The differential cross section for the t channel QED process, $e^+e^- \to (e^+)e^-\gamma$, was calculated to be,

$$d^5\sigma = \frac{\alpha^3}{\pi^2 s}\left(s^2 + s'^2 + u^2 + u'^2 + \frac{8m_e^2}{t}(x_2^2 + y_2^2)\right)\left(\frac{-1}{x_2 y_2 t}\right) d^5\Gamma$$

The notation is that of Berends and Kleiss.[1] A Monte Carlo program was written to simulate this process near the t pole (a region where the Berends and Kleiss Monte Carlo was not intended to function). The total cross section and invariant mass distribution agrees with a calculation using the equivalent photon approximation.[2]

This new Monte Carlo was used to generate events, with the $e\gamma$ in the region $|\cos\theta| < 0.75$ and the other e in the region $\theta < 100$ mrad. After detector simulation and analysis, the invariant mass distribution was fit with a 6^{th} order Legendre polynomial, to define the QED background.

The e^* production cross section was calculated using the following low energy effective Lagrangian,[3]

$$\mathcal{L}_{eff} = \left(\frac{e}{2}\right)\left(\frac{\lambda}{m_{e^*}}\right)\overline{\psi}_{e^*}\sigma_{\mu\nu}\psi_e F^{\mu\nu} + h.c.$$

where λ/m_{e^*} is the coupling constant at the $e\gamma e^*$ vertex.

Monte Carlo generated e^* events were run through the detector simulation and analysis to find the resolution and efficiency for various values of m_{e^*}. The typical resolution is 100 MeV/c^2.

Results

The $e\gamma$ events were selected by requiring one charged and one neutral track with $|\cos\theta| < 0.675$ and at most one track in the small angle tagger (SAT), which covers $21 < \theta < 81$ mrad.

Background contributions from mistracked Bhabhas, photon conversion and higher order QED were reduced with the following criteria: Drift chambers hits do not indicate a

missed prong or converted photon; acollinearity of the $e\gamma$ > 20 mrad; the event plane is less than 80 mrad from the beam pipe for events without a SAT track; in a constrained fit, the event should be consistent with a three body final state. The effectiveness of these cuts against the background is seen in the $e\gamma$ visible energy distribution (Fig. 1).

The energies of the electrons and photons were determined using angular measurements alone by assuming a three body final state. The energies calculated in this way have a typical resolution of 75 MeV, whereas the calorimetric measurements have a typical resolution of 450 MeV.

From the QED Monte Carlo studies, 3377 events are expected in the data sample of 211 ± 11 pb^{-1}, while only 3034 events are seen; about 11% low. A deviation is not unexpected since radiative corrections have not yet been applied. However, the overall normalization does not affect the limits on the e^* coupling strength, since this involves an analysis of the shape of the $e\gamma$ invariant mass distribution.

Figure 2 shows the $e\gamma$ invariant mass distribution and the normalized QED Monte Carlo curve, which are in good agreement. Also shown are the limits on the coupling constant, λ/m_{e^*}, as determined from a likelihood analysis. A corresponding limit on the substructure scale, Λ_{Sub}, depends on the parameterization of the coupling constant. If the coupling constant is written as $1/\Lambda_{Sub}$, then $\Lambda_{Sub} \geq 3$ TeV. However, if it is instead written as m_{e^*}/Λ^2_{Sub}, as suggested from chiral symmetry arguments,[4] then $\Lambda_{Sub} \geq 300$ GeV. These limits are only valid for $14 < m_{e^*} < 28.5$ GeV/c^2.

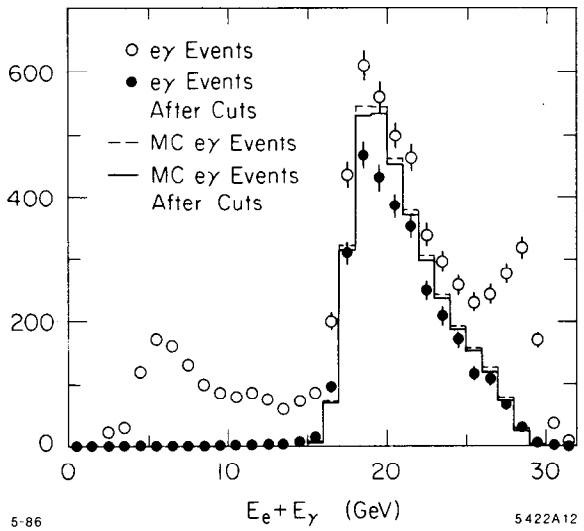

Fig. 1. Visible energy distribution of the $e\gamma$ events before and after the cuts against background. Histogram: Monte Carlo; Points: Data.

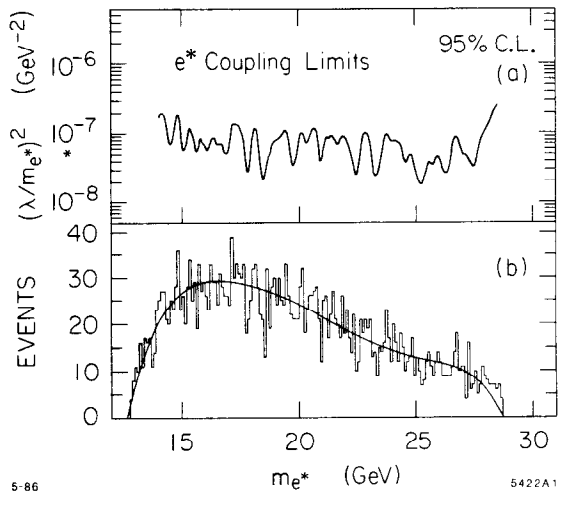

Fig. 2. $e\gamma$ invariant mass distribution with QED Monte Carlo curve and corresponding limits on the coupling strength (preliminary).

2. Searches for Weakly Interacting Particles

This section reports on a search for the production of new particles that interact only weakly in matter. Since these particles are not directly observable this is done by searching for the radiative production of these particles.

This search is of particular interest for supersymmetry (SUSY) theories. These theories postulate the existence of a new class of particles: supersymmetric partners of ordinary particles different only in spin by 1/2 unit. Photinos ($\tilde{\gamma}$) and sneutrinos ($\tilde{\nu}$) are examples of weakly interacting particles that may be light and could be produced in e^+e^- annihilation. Because of a conserved quantum number the lightest SUSY particle is stable; cosmological arguments indicates that this particle is probably neutral. It is generally assumed that this particle is a fermion since they may be protected by chiral symmetry from becoming massive during the supersymmetry breaking.

An established type of weakly interacting particle produced in e^+e^- annihilations is the neutrino. The form of the cross section of the radiative production of neutrinos in the local limit ($\sqrt{s} \ll m_W$), is given by:

$$\frac{d\sigma(e^+e^- \to \gamma\nu\bar{\nu})}{dE_\gamma d\cos\theta_\gamma} \sim \frac{\alpha}{p_t^\gamma \sin\theta_\gamma} \cdot \frac{\alpha^2 s}{m_W^4 \sin^4\theta_W} \cdot (1 + N_\nu/4) \quad , \tag{1}$$

The first factor indicates the dependency of the radiative correction on p_t^γ, the momentum transverse to the beam axis, and θ_γ, the polar angle of the radiated photon. The factor $(1 + N_\nu/4)$ contains the relative strength of the charged and neutral weak currents. For $\sqrt{s} \sim m_{Z^0}$ the cross section will be dominated by the neutral current channel is and almost proportional to the number of neutrinos. For PEP energies the finite width of the Z^0 pole has the effect of giving the cross section an $1 + N_\nu/2.7$ dependency. The cross section for $N_\nu = 3$ and integrated over $x_\gamma > 0.2$ as a function of the center of mass energy is shown in Fig. 3. As suggested by Ma and Okada,[5] this process provides a method of counting the number of neutrinos species without any assumption other than the standard model coupling of the Z^0 to a single family.

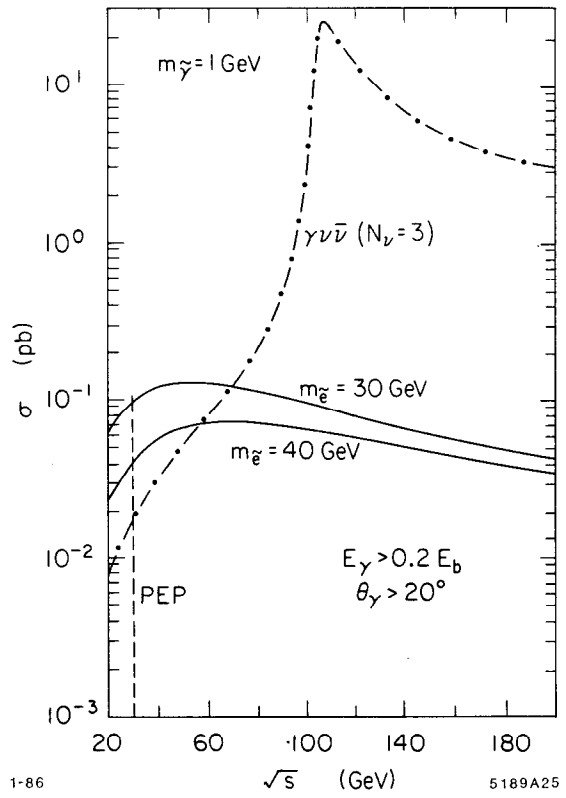

Fig. 3. Comparison of cross sections for $\gamma\nu\bar{\nu}$ and $\gamma\tilde{\gamma}\tilde{\gamma}$.

Fayet[6] and others,[7] have pointed out that if the photino is light, a search for single photon states is also a particularly sensitive way of testing supersymmetry. The cross section of radiative production of photinos in the limit $\sqrt{s} \ll m_{\tilde{e}}$ can be expressed in a form similar to (1) by:

$$\frac{d\sigma(e^+e^- \to \gamma\nu\bar{\nu})}{dE_\gamma d\cos\theta_\gamma} \sim \frac{\alpha}{p_t^\gamma \sin\theta_\gamma} \cdot \frac{\alpha^2 s}{m_{\tilde{e}}^4} \, , \tag{2}$$

where $m_{\tilde{e}}$ is the mass of the spin zero partner of the electron (selectron). This cross section is shown in Fig. 3 along the cross section of radiative neutrino production for comparison.

This figure shows that a SUSY search at higher energies is limited by background from ($\gamma\nu\bar{\nu}$) production and that at PEP energies higher sensitivity for the mass of the selectron can be obtained.

Single Photon Detection

Since the radiative cross section depends on $1/p_t^{\gamma}$ and $1/\sin\theta_\gamma$, good photon detection efficiency down to small values of p_t^{γ} and θ_γ is desirable. In addition it is also necessary to show that the detected events are accompanied only by weakly interacting particles, requiring complete solid angle coverage with electromagnetic calorimetry and charge particle tracking. The largest background comes from the radiative Bhabha process, $e^+e^- \rightarrow ee\gamma$, and requires a rejection of $\sim 10^{-4}$ to reach a sensitivity to neutrino pair production. Using the kinematics of the three body final state, this rejection is fully obtained by a complete veto capability for $\theta > \theta_{veto} = p_{t\,min}^{\gamma}/2E_{beam}$. The detection and kinematical reconstruction of these events also provides an excellent source of "tagged" single photons, to test and calibrate the experimental technique of the signal extraction.

Another background to the single photon sample at low p_t comes from π^0's produced in beam gas interactions. In order to reject this background one needs a high efficiency for detecting beam gas residuals. This requires a quiet detector (so very low veto limits may be applied) and preferentially no magnetic field (so that low energetic particles, which would otherwise be curled up in the beam pipe, can be detected). Good reconstruction of the photon origin along the beam direction will help further reduce this background.

Single Photon Detection with the ASP Detector

The ASP apparatus (Fig. 4) was specially designed to detect single photons. Photons produced at angles $20° < \theta_\gamma < 160°$ are detected in five-layer stacks of lead-glass bars which completely surround the interaction point (I. P.) in azimuth. The bars are staggered along the beam direction to eliminate cracks and to provide optimal resolution of the origin of electromagnetic showers. The energy resolution of the calorimeter is measured with radiative Bhabha events to be 15% at 1 GeV when averaged over all angles with $\theta > 20°$. The lead-glass layers are interleaved with proportional wire chambers (PWCs) to provide position information in the plane perpendicular to the beam. Charged particles are tracked between the beam pipe and central calorimeter by planes of proportional tubes parallel to the beam line. The central tracker is surrounded by 2 cm thick veto scintillators.

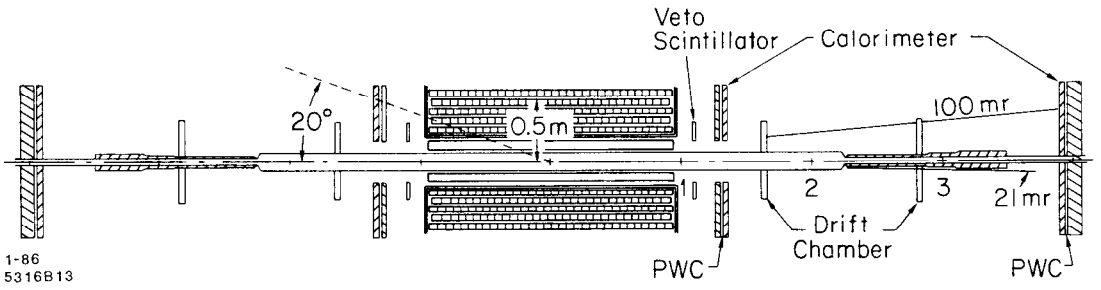

Fig. 4. View along the beam axis of the ASP detector. The apparatus is approximately 8 meters long and 1 meter wide.

Calorimeter modules made from lead and scintillator surround the beam pipe in the forward angle region. Proportional tubes measure the spatial positions of showers at a depth of $6X_0$ in these modules. The forward calorimeter modules overlap each other and the central calorimeter so that no gaps occur in the detector for $\theta > 21$ mr.

The detector is located 20 m underground. This filters all primary hadrons from the cosmic ray flux and reduces the overall intensity by a factor of ≈ 2.7. Scintillation counters above the detector provide an additional order of magnitude rejection of cosmic rays.

Signals from the lead-glass bars are electronically summed and discriminated to generate hardware triggers. The single photon trigger is based on several such sums and, using the $ee\gamma$ event sample, is measured to be $> 99\%$ efficient for single photons in the fiducial region of the signal: $p_t^\gamma > 1$ GeV/c and $\theta_\gamma > 20°$. Signals from the forward shower modules are used to trigger on small angle Bhabha scattered electrons. A special trigger for radiative Bhabha ($ee\gamma$) events is formed by placing the small-angle Bhabha trigger in coincidence with a very low (≈ 0.2 GeV) threshold on the total lead-glass pulse height.

ASP Data

The results presented in this section have been previously published.[8] Photon candidates were selected from the ASP data sample of 68.7 pb^{-1} by requiring a cluster of lead glass bars whose pattern is consistent with photon patterns as determined with the $ee\gamma$ sample. Cosmic ray induced background was eliminated by requiring the time of the event (determined by the lead-glass energy sums) to be within 3σ of the beam crossing time and by the requirement that the projected distance of closest approach of the shower in the XY plane is less than 20 cm. The efficiency of all of these cuts is measured to be 75% with little dependency on E_γ and θ_γ.

The ability to isolate a single photon-state from the background depends upon the noise levels and occupancies in the components of the detector. Random triggers are used to determine the efficiency for the veto cuts, while $ee\gamma$ events were used to study the occupancies which are correlated with the presence of a photon (e.g. caused by backsplash or leakage). The efficiency for all veto cuts is determined to be 60%, with the cuts arranged so that no single component of the detector contributes an inefficiency greater than 10%.

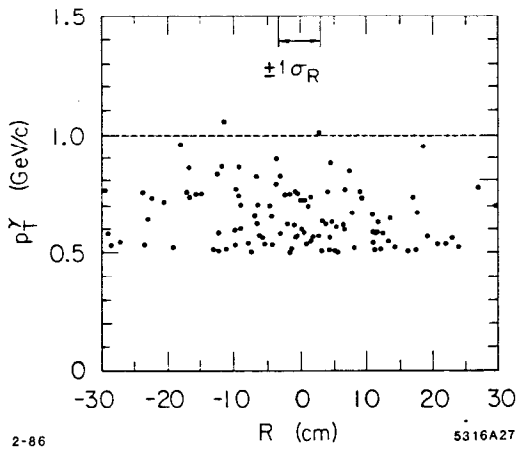

Fig. 5. Final sample of single-photon candidates with $p_t^\gamma > 0.5$ GeV/c and $\theta_\gamma > 20°$.

The remaining single photon candidates with $p_t > 0.5$ GeV/c and $R_0 < 30$ cm (the distance of closest approach in the shower projection measured by the lead-glass system) are shown in Fig. 5 as a function of p_t^γ and R_0. The resolution in R_0 for single photons was determined using the $ee\gamma$ sample to be gaussian with $\sigma = 3$ cm and an exponential tail. Since the photon pattern recognition cuts are biased towards events coming from the origin, the R_0 distribution for the background is not flat. This shape was determined, by relaxing cuts

other than these pattern cuts, to be gaussian with a $\sigma = 12$ cm.

With the R_0 shape information for signal and background a likelihood analysis of the two events with $p_t^\gamma > 1$ GeV/c was made to determine the upper limit for the number of signal events. The limits are 2.9 and 3.9 events for 90% and 95% confidence level respectively.

Using the measured luminosity and photon efficiency an upper limit on the sum of *all* contributions to the single photon cross section can be calculated for the ASP search region: $\sigma < 0.094$ pb. This limit allows for a maximum of 14 neutrino families (90% C.L.).

The cross section[9] for radiative production of three neutrino species with photons in the ASP acceptance is 0.032 pb, corresponding to one expected event. Hence the sum of all non-standard model contributions must be less than 0.062 pb. From the exact cross section[10] for $e^+e^- \to \gamma\tilde{\gamma}\tilde{\gamma}$ we deduce the corresponding limits shown in Fig. 6 on the $\tilde{e}$ and $\tilde{\gamma}$ masses. For massless photinos the 90% C.L. limit on the selectron mass is $m_{\tilde{e}} > 51$ GeV/c^2 ($m_{\tilde{e}_L} = m_{\tilde{e}_R}$) and $m_{\tilde{e}} > 51$ GeV/c^2 ($m_{\tilde{e}_L} \ll m_{\tilde{e}_R}$).

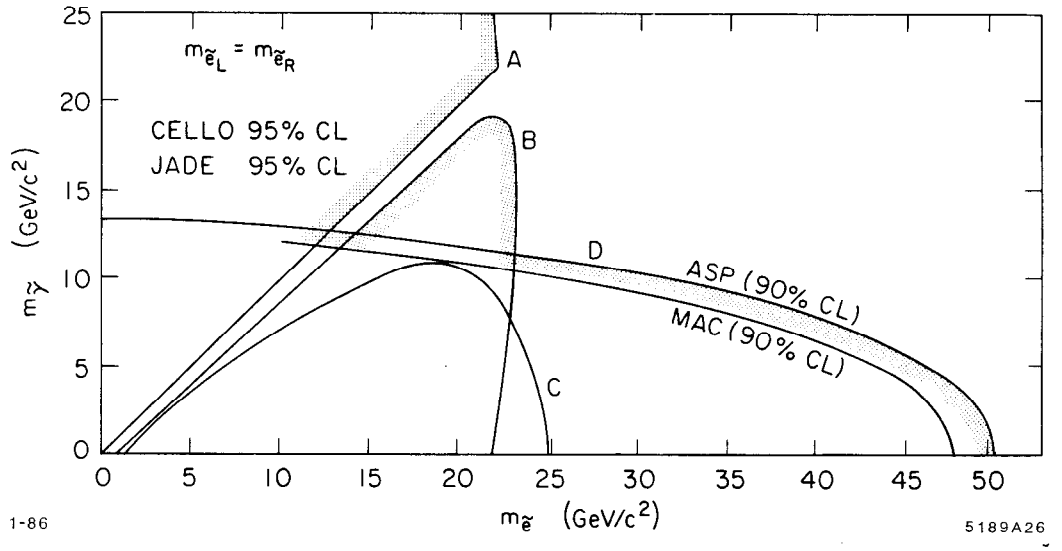

Fig. 6. Summary of limits on $m_{\tilde{e}}$ and $m_{\tilde{\gamma}}$. Curve A: stable massive charged particles. Curve B: acoplanar e^+e^- pairs. Curve C: single electron production. Curve D: single photon production.

MAC Data

The MAC collaboration published an earlier result[11] on the single photon analysis based on a sample of 116 pb^{-1}. In this talk a new result is given based on an enlarged data sample of 177 pb^{-1} and an improved analysis. The new analysis makes a complete use of all small angle detectors and makes more stringent requirements on the photon origin and energy deposition pattern. The search region for the MAC detector is defined by $40° < \theta_\gamma < 140°$. The p_t cut on the photon was determined by the forward veto capabilities of the detector in each running period. In the first period (36 pb^{-1}) with $\theta_{veto} > 10°$ the cut $p_t > 4.5$ GeV/c was applied; the second period (80 pb^{-1}) with $\theta_{veto} > 2.5°$ $p_t > 2.0$ GeV/c; while the last period (61 pb^{-1}) with $\theta_{veto} > 4.8°$ used the cut $p_t > 2.6$ GeV/c. The expected yield of photons from $e^+e^- \to \nu\bar{\nu}\gamma$ ($N_\nu = 3$) in the combined search regions is 1.1 event. The relative sensitivity of each data sample is best expressed in the expected number of events in each

period: 0.1, 0.6 and 0.4 . One event was observed at $p_t = 5.3$ GeV/c, which corresponds to a limit on $N_\nu < 17$ at 90% confidence level. The corresponding region of excluded $\tilde{e}\tilde{\gamma}$ masses are shown in Fig. 6. For $m_{\tilde{\gamma}} = 0$ the 90% C.L. limits are $m_{\tilde{e}} > 48$ GeV/c^2 ($m_{\tilde{e}_L} = m_{\tilde{e}_R}$) and $m_{\tilde{e}} > 40$ GeV/c^2 ($m_{\tilde{e}_L} \ll m_{\tilde{e}_R}$).

Limits on Other SUSY Particles

If the lightest supersymmetric particle is the sneutrino then a limit on single photon production constrains the mass of the wino. Using the ASP result and a model for sneutrino production[12] adapted for initial state radiation, the 90% C.L. limit on the mass of the wino is $m_{\tilde{W}} > 48$ GeV/c^2. In this calculation the assumptions of massless sneutrinos, no mixing between the wino and higgsinos, and only one light wino ($m_{\tilde{\nu}} = 0$, $O^+ = 1$, and $m_1 \ll m_2$) have been made. Using a different model[13] the MAC collaboration calculates a similar result, $m_{\tilde{W}} > 50$ GeV/c^2.

Finally, if one assumes that at some scale the gauge couplings for strong and electromagnetic interactions become equal and at that scale the squarks and sleptons are related by $m_{\tilde{q}} = m_{\tilde{e}}$, then the relations between these masses can be calculated at any scale. In particular, at present energies we would have[14]

$$m_{\tilde{g}} \simeq \frac{3}{8}\frac{\alpha_s}{\alpha_{em}} m_{\tilde{\gamma}} \simeq 6.3 m_{\tilde{\gamma}} \quad \text{and} \quad m_{\tilde{q}}^2 \simeq 32 m_{\tilde{\gamma}}^2 + m_{\tilde{e}}^2 \quad .$$

Using these relations, the ASP excluded region can be mapped into the squark, gluino mass plane. The excluded region is shown in Fig. 7 together with approximate limits determined from a theoretical analysis of monojet searches[15] and cosmological constraints.[16,17]

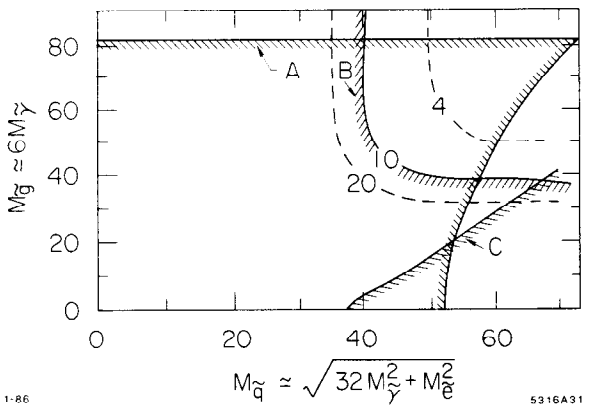

Fig. 7. The excluded region in $m_{\tilde{g}}$ and $m_{\tilde{q}}$ from (A) ASP, (B) monojets and (C) cosmology.

REFERENCES

1. F. Berends and R.Kleiss, *Nucl. Phys.* **B228** (1983), 537.
2. A. Courau and P. Kessler, *Phys. Rev.* **D33** (1986), 2024.
3. F.E. Low, *Phys. Rev. Lett.* **14** (1965), 238.
4. M.E. Peskin, *1985 International Symposium on Lepton and Photon Interactions at High Energies*, Kyoto, Japan, SLAC-PUB-3852.
5. E. Ma and J. Okada, *Phys. Rev. Lett.* **41** (1978), 287; K. Gaemers, R. Gastmans and F. Renard, *Phys. Rev.* **D19** (1979), 1605.
6. P. Fayet, *Phys. Lett.* **117B** (1982), 460.
7. J. Ellis and J. Hagelin, *Phys. Lett.* **122B** (1983), 303.
8. G. Bartha *et al.* (ASP collaboration), *Phys. Rev. Lett.* **56** (1985), 685.
9. K.J.F. Gaemers, R. Gastmans, and F.M. Renard, *Phys. Rev.* **D19** (1979), 1605.
10. K. Grassie and P.N. Pandita, *Phys. Rev.* **D30** (1984), 22.
11. E. Fernandez *et al.* (MAC Collaboration), *Phys. Rev. Lett.* **54** (1985), 1118.
12. J.S. Hagelin, G.L. Kane and S. Raby, *Nucl. Phys.* **B241** (1984), 638.
13. J.A. Grifols, M. Martinez, and J. Sola, *Nucl. Phys.* **B268** (1986), 151.
14. M. Sher, private communication with R. Hollebeek; J. Polchinski, *Phys. Rev.* **D26** (1982), 3674.
15. J. Ellis, *1985 International Symposium on Lepton and Photon Interactions at High Energies*, Kyoto, Japan, CERN-TH-4277/85.
16. H. Goldberg, *Phys. Rev. Lett.* **50** (1983), 1419.
17. J. Ellis, J. Hagelin, D. Nanopoulos, K. Olive and M. Srednicki, *Nucl. Phys.* **B241** (1984), 381.